# UNCERTAINTIES IN RISK ASSESSMENT OF HYDROGEN DISCHARGES FROM PRESSURIZED STORAGE VESSELS AT LOW TEMPERATURES

**Markert, F.[1], Melideo, D.[2] and Baraldi, D.[2]**
**[1] Department of Management Engineering, Technical University of Denmark, Produktionstorvet 424, Kongens Lyngby, 2800, Denmark, fram@dtu.dk**
**[2] Institute for Energy and Transport, Joint Research Centre European Commission, Westerduingweg 3, Post box 2, Petten, 1755 ZG, Netherlands, daniele.melideo@ec.europa.eu, daniele.baraldi@jrc.nl**

**ABSTRACT**

Evaluations of the uncertainties resulting from risk assessment tools to predict releases from the various hydrogen storage types are important to support risk informed safety management. The tools have to predict releases from a wide range of storage pressures (up to 80 MPa) and temperatures (at 20K) e.g. the cryogenic compressed gas storage covers pressures up to 35 MPa and temperatures between 33K and 338 K. Accurate calculations of high pressure releases require real gas EOS. This paper compares a number of EOS to predict hydrogen properties typical in different storage types. The vessel dynamics are modeled to evaluate the performance of various EOS to predict exit pressures and temperatures. The results are compared to experimental data and results from CFD calculations.

## 1.0 INTRODUCTION

Hydrogen may be thermodynamically considered as an ideal gas over a very wide temperature and pressure range. Nevertheless, present technological developments stores hydrogen in the liquid state at about 20K under a low pressure of few bars and in the gaseous state at very high pressures up to 800 – 1000 bars at ambient temperatures. Recently, the operational regime of cryo compressed hydrogen (CcH2) storage was reported to cover pressures of up to 35 MPa and temperatures from 338K down to 33K [1,2]. Considering these wide ranges for temperature and pressures, the assumption of ideal gas behavior and application of the ideal gas equations of state (EOS) is not adequate for all situations. This has been recognized by the scientific community and different approaches describing high pressure gas releases at ambient conditions from storage tanks [3-7] and within vehicles [8] are described. This discrepancy of behavior between ideal gas and real gas is illustrated in Figure 1, where the state-of-the-art reference data provided by NIST[1] [3] are compared against predictions using the EOS for ideal gas. It is shown that the ideal gas EOS accuracy in predicting the density pressure relationship is limited up to about 35MPa at 500K, and up to about 15MPa at 200K.

From the risk assessment point of view a large number of release scenarios have to be analyzed, to give a comprehensive evaluation of the associated risks and to provide useful data for risk management purposes. In many scenarios at ambient conditions and moderate storage pressures the use of engineering equations based on the ideal gas EOS may give sufficiently accurate results to make proper decisions. For analyzing accident scenarios for very high pressure and cryogenic storage cases real gas behavior of the hydrogen needs to be taken into account to reduce the level of uncertainty in the evaluations. For this purpose several EOS are being developed, which may be classified into the cubic EOS type[2)] (equations by e.g. Abel-Nobel[3]; van-der-Waals; Redlich-Kwong; Redlich-Kwong-Soave; Peng-Robinson; Beatty-Bridgeman) using corrections for the gas volume and pressure assuming the finite volume of the molecules and the intermolecular forces, respectively. The

[1] Accesible from http://webbook.nist.gov/chemistry/fluid "hydrogen" and described in the PhD thesis by Leachman: http://www.boulder.nist.gov/div838/theory/refprop/leachman.pdf
[2] http://en.wikipedia.org/wiki/Equation_of_state#Cubic_equations_of_state
[3] The Abel-Nobel EOS only assumes corrections to the finite volume of the molecules

accuracy of these to predict the temperature- pressure behavior at constant density of 11.6 mol/L, which is the density of hydrogen in a 35 MPa pressurized storage at ambient temperatures, is illustrated in Figure 2. Recently, eleven expressions of the cubic EOS family have been reviewed on their accuracy predicting various supercritical properties of hydrogen by Nasrifar [9].

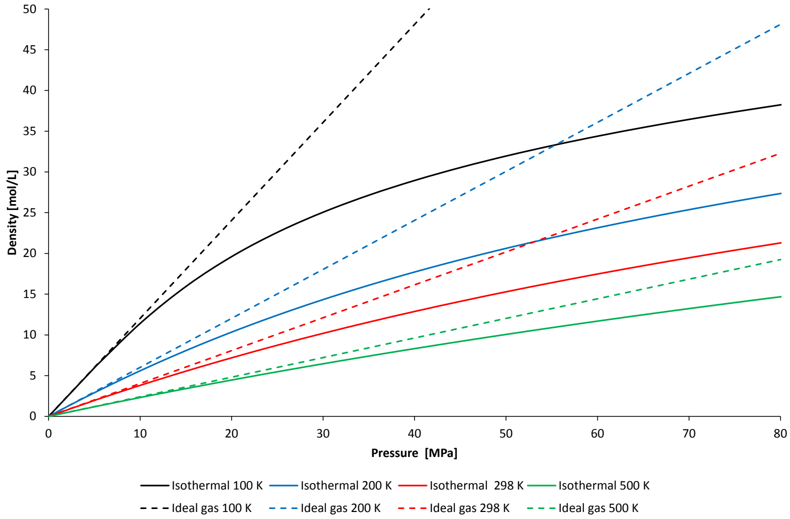


Figure 1. Real gas behaviour for some isotherms (continuous line) compared to ideal gas behaviour (dotted lines).

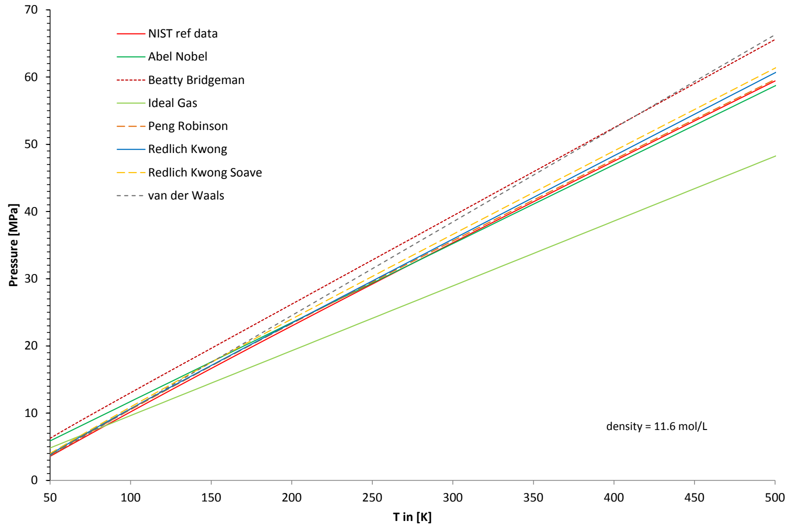


Figure 2. Isochoric temperature –pressure plots for 11.6 mol/L (equal to about 35MPa at ambient temperature) showing the accuracy of some cubic EOS compared to the NIST data and the ideal EOS

The authors are not aware of release experiments in the low temperature range, but with the findings described above, it is important to address such releases. This paper is a first theoretical analysis to identify the potential uncertainty in the predictions of hydrogen releases at low temperatures and to evaluate the possible effects to overall hydrogen safety using the correlations on jet flame length by Saffers and Molkov [10] and correlations on explosion severity by Dorofeev [11].

## 2.0 THEORETICAL BACKGROUND

For risk assessment purposes, it may be sufficient to know the initial vessel conditions, e.g., using the initial mass release, which is the maximum rate in any release, to take a conservative approach. In the case, where more detailed release scenarios are required, a time dependent approach has to be taken into account to predict mass release rate decays. Hereunder, it is important to know about parameters like vessel temperature, vessel pressure, throat pressure and sonic speed of the released gas that determine jet properties and jet flames. Therefore, models need to be capable of predicting such parameters. This paper will focus on the accuracy to model time dependent vessel pressures and temperatures and mass release.

Several EOS are applied to calculate the mass release rate at ambient (300 K) and low (200 K) temperatures at two vessel pressures (30 and 34.5 MPa). The implementation of the real gas properties is implemented using the compressibility factor Z (see appendix A). The temperature profile in the vessel as well as important release parameters are calculated using an engineering numerical model called "DTU analytical model" in the following. It is developed to predict vessel dynamics and it is based on a model description from the Yellow book (see appendix A and CPR 14E chapter 2.5.2.2; [12] ) and a CFD model [7] using on the one side the ideal gas EOS and selected cubic EOS. The results are compared to former findings by Mohamed and Paraschivoiu [13].

There are a great number of articles describing pressurized releases at ambient temperatures at moderate pressures. In such scenarios the specific heat ratio $C_p/C_v$ is only slightly dependent on temperature and pressure as shown in Figure 3 for 298K and 500K. For lower temperatures, also shown in Figure 3, an increasingly stronger dependency on pressure is observed for $C_p/C_v$. Also in Figure 3, the pressure dependency of the isochoric heat capacity $C_v$ is shown for a number of temperatures, and as the dependency of $C_v$ is close to linear, it is obvious that the pressure dependency for $C_p$ is becoming strongly non-linear at low temperatures. Furthermore Figure 3 (top right) shows isochoric data for the temperature dependency of $C_p$ and $C_v$ for densities ranging from 2 – 21.3 mol/L. It is seen that the temperature dependence of the $C_v$ values are only slightly altered by pressure. Therefore, the DTU analytical model predicts the temperature variation within the vessel by using $C_v$ values from a fit to the original data at one density in the temperature interval relevant for the calculations.

Being a diatomic linear molecule, hydrogen has three translational and two rotational degrees of freedom contributing to its specific heat capacity. Thus, hydrogen's theoretical predicted specific heat capacity $C_v$ is close to 2.5R= 20.785 J $mol^{-1}K^{-1}$, as it is actually observed at 500 K and 298 K with 20.953 and 20.47 J $mol^{-1}K^{-1}$, respectively. With decreasing temperatures the value of the specific heat capacity $C_v$ is falling approaching the theoretical value for monatomic gases (three degrees of freedom) of 1.5R= 12.471 J $mol^{-1}K^{-1}$. Thus, at low temperatures, hydrogen is thermodynamically behaving as a monatomic gas, which is caused by quantum effects reducing the number of possible rotational energy levels. The rotational energy level gap is getting much larger than kT [4)] at 60 K[5)] and, by that, the two rotational energy levels are decreasingly less populated with decreasing low temperatures. The onset temperature for this quantum effect is T< 160K according to [9]. Additional findings and references may be found in [14].

*Table 1. Linear fit to $C_v$ plots in Figure 3 (shown (right bottom) as dotted lines)*

| T K | $C_v$-slope | $C_v$ ideal | $R^2$ |
|---|---|---|---|
| 500 | 0.0088 | 20.953 | 0.9992 |
| 298 | 0.0152 | 20.47 | 0.9984 |
| 200 | 0.0213 | 19.023 | 0.9966 |
| 150 | 0.0271 | 17.165 | 0.9926 |
| 100 | 0.0336 | 14.525 | 0.9756 |

[4] kT is an energy level with k being the Boltzmann constant and T the absolute temperature
[5] Chapter 8; Heat capacity and the expansion of gases (page 5) orca.phys.uvic.ca/~tatum/thermod/thermod08.pdf

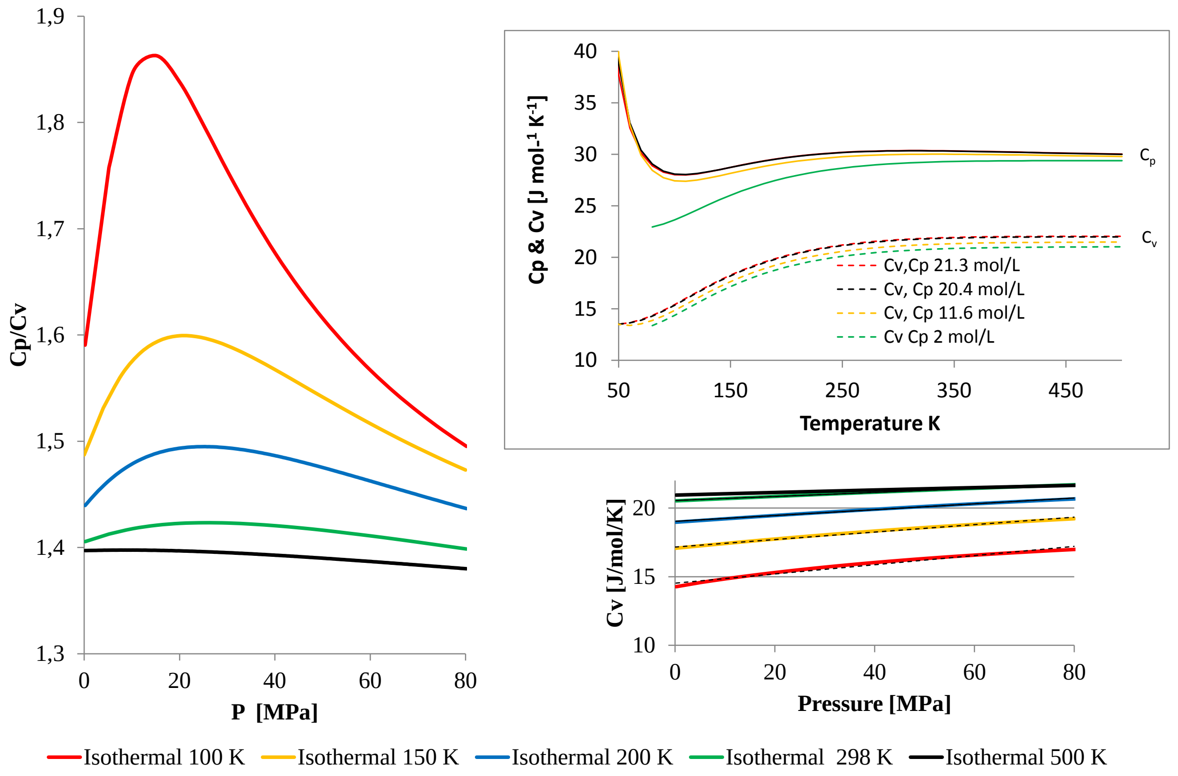


Figure 3. Real gas behaviour of normal hydrogen: $C_p/C_v$ vs. pressure at several isotherms. Also shown (small figure right bottom) $C_v$ versus pressure at the same isotherms. The dotted lines are linear fits to the graph and the respective coefficients are listed in Table 1. Also shown are isochoric data (right top) for the temperature dependency of $C_p$ and $C_v$ are shown for densities between 2 - 21.3 mol/L.

## 3.0 THE CASE STUDY

### 3.1 Engineering modeling strategy

The following three cases are modeled by the DTU analytical model and the results are compared with the JRC CFD release model. For validation purposes, the first case is equal to the configuration in Mohamed and Paraschivoiu's paper [13]. The release is from a hole with a radius of r=3.18mm in a 27 L cylindrical tank. The initial tank pressure is 34.5 MPa at a temperature of 300 K. Mohamed and Paraschivoiu used the Beattie-Bridgeman EOS and a 3-D unstructured tetrahedral finite volume Euler solver to model a high pressure hydrogen release at ambient temperature. They additionally applied an analytical model with the following assumptions: the thermodynamic properties are uniform in the tank; the release occurs at adiabatic conditions; the release is sonic at the orifice (velocity of gas is equal to the local speed of sound); the expansion of hydrogen from the stagnation state in the vessel to the critical state at the orifice takes place in a small region near the orifice being modeled as quasi one-dimensional isentropic flow. These assumptions for the analytical model are essentially the same as used in the DTU analytical model. In the second case, the geometry is kept unchanged while the initial pressure and temperature are equal to 30MPa and 200K respectively. In the third case, a much larger tank was considered (197L and 5.7mm orifice radius) with the same initial conditions like in case 2.

### 3.2 CFD modeling strategy

The ANSYS CFX14.0 fully compressible solver was used [15]. Hybrid axy-simmetric meshes were generated with Pointwise 17.0 [16] as shown in Figure 4. The mesh is a pseudo 2-dimensional mesh since it is one cell thick in the y direction and it represents 1/360 of the whole 3D geometry. The main domain in the tank is built with an unstructured tetrahedral mesh. Since in the leak a preferential direction in the movement of the flow can be easily identified, a structured mesh was generated in that region. In the validation case with the 27 L tank, two computational grids were built in order to investigate the grid independence. The number of nodes in the meshes is reported in Table 3. It must be emphasized that the number of nodes is reported instead than the number of cells because in ANSYS-CFX the control volumes are built around the nodes and therefore their number is equal to the number of nodes. Negligible differences were observed in the results between the two grids. The high resolution advection scheme and the second order backward Euler time scheme were selected. The free slip boundary condition is applied to the walls and the exit surface is modeled as a supersonic outlet boundary condition, following the modeling strategy by Mohamed and Paraschivoiu [13].

Table 2. Selected scenarios

| | Tank volume (L) | Orifice diameter (mm) | Initial pressure (MPa) | Initial temperature (K) |
|---|---|---|---|---|
| case 1 (Validation) | 27 | 3.18 | 34.5 | 300 |
| case 2 | 27 | 3.18 | 30 | 200 |
| case 3 | 197 | 5.7 | 30 | 200 |

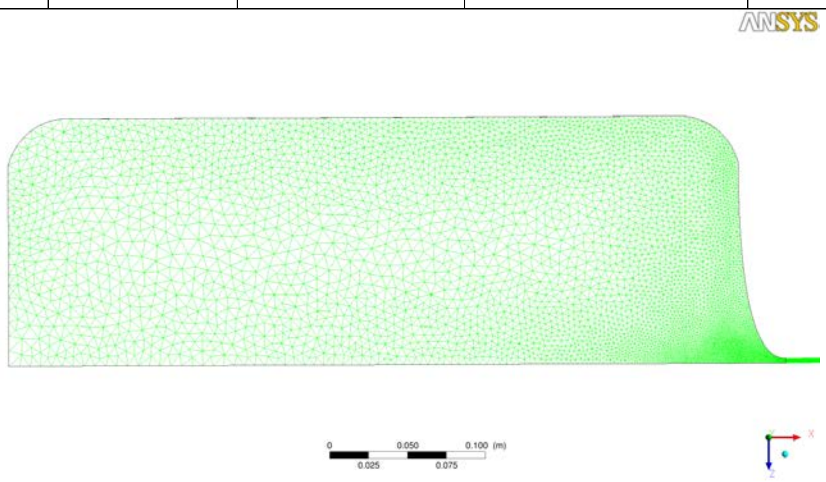

Figure 4: Computational mesh.

Table 3: Number of nodes in the computational grids.

| Mesh | Number of nodes |
|---|---|
| 27 L coarse | 2984 |
| 27 L fine | 13380 |
| 197 L | 7328 |

## 4.0 RESULTS

### 4.1 Case 1: 27 L vessel at ambient conditions (300 K)

Simulations are performed for the ideal gas release, the CFD code using the Peng Robinson EOS and the engineering model using Leachman's EOS adaption for the compressible factore Z [3,17]. In the engineering model, the specific heats are varied: 1) $C_v$ and $C_p$ taken as constant at initial vessel temperature; 2) $C_v$ and $C_p$ taken as constant at $(T_{end}-T_{start})/2$ and finally 3) as a function of the temperature $C_v(T)$ and $C_p(T)$. Furthermore, the results are compared to the ones published by Mohamed et al. [13] using an analytical and a 3D CFD approach.

At ambient conditions the ideal gas calculations compare excellent with eachother. The real gas EOS models provide very similar results for the mass flow decay, the pressure decay in the vessel and the temperature decay in the vessel, though there are some uncertainties observed using the real gas EOS below 20 MPa vessel pressures and the corresponding release rates. Here Beatty-Bridgeman deviates somewhat from the Peng-Robinson and NIST based calculations. The ideal gas approach is calculating the same release duration as the real gas EOS estimations and the initial releases are about the same for all. Nevertheless, the pressure and mass flow rate decay quicker for the real gas estimations.

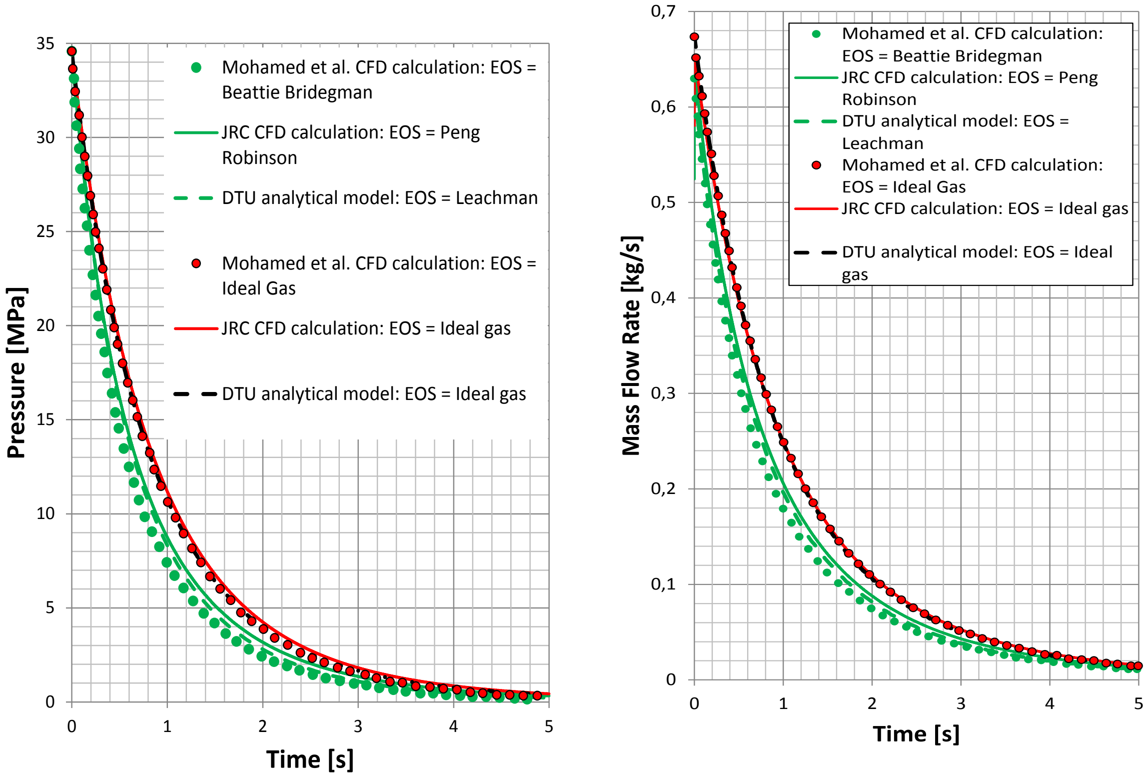


Figure 5. Release calculations at 300K and a vessel pressure of 34.5MPa. The hole-radius is 3.18mm. The JRC CFD calculation and the DTU analytical model are compared with the CFD calculations by Mohamed et al..

#### 4.2 Case 2: 27 L vessel at low temperature (200 K)

Simulations are carried out for the ideal gas release, the CFD code using the Peng Robionson EOS and the engineering model using Leachman's EOS adaption for the compressible factor Z [3,17]. The specific heats are varied: 1) $C_v$ and $C_p$ taken as constant at initial vessel temperature; 2) $C_v$ and $C_p$ taken as constant at $(T_{end}-T_{start})/2$ and finally 3) as a function of the temperature $C_v(T)$ and $C_p$ (T). In Figure 7 the results for the mass release shows the highest release for the ideal gas approximation being thus a conservative approach. The initial rates are about the same for all simulations. The models using the real gas predictions give about the same results. Similar findings are valid for the vessel pressure time profile. The temperature of the gas in the vessel is predicted considerably different comparing the three EOS applied. It further shows that the approximation of $C_v$ and $C_p/C_v$ is important to chose as some differences are observed. Due to the lack of experimental data it is not possible to predict the real temperature decay and giving recommendations on the best approach for predictions. The sound velocity has been calculated as seen in Figure 7.

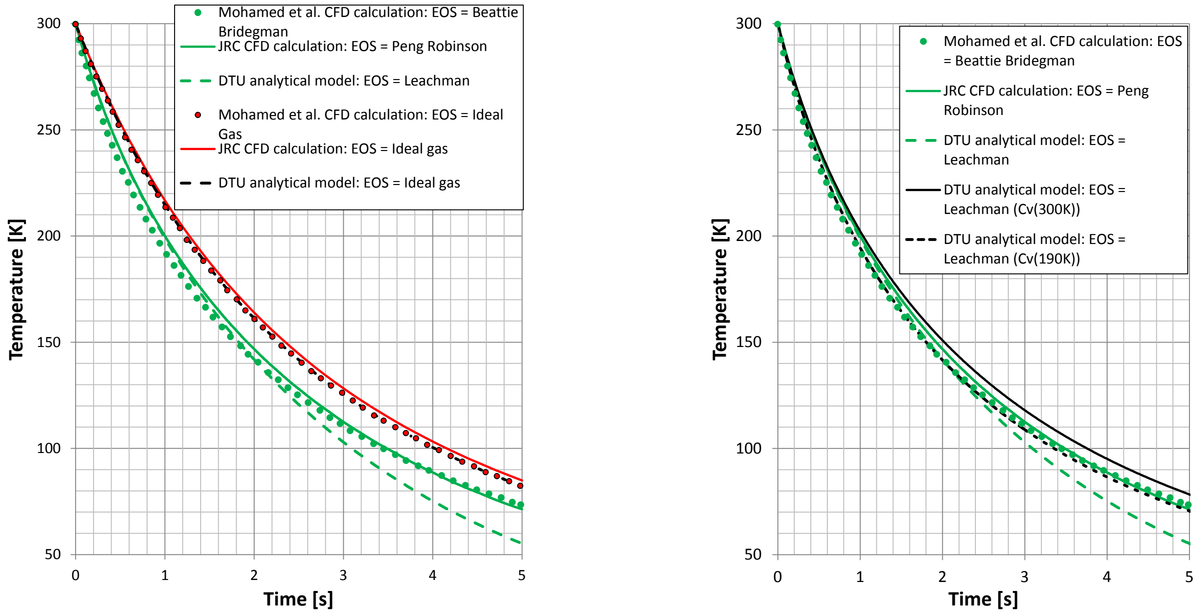


Figure 6.Case1: Comparing ideal and real gas temperature profiles at ambient conditions. For real gas EOS profiles of the vessel temperature using Beattie Bridgeman (Mohamed et al.), Peng Robinson (JRC CFD) and Nist/Leachman (DTU analytical model). As shown on the left. On the right the results of a $C_v$ variation are shown, as a) function of temperature, b) constant value $C_v$ at 300K (solid black line) and c) constant value $C_v$ at 190K ($T_{end}$-$T_{start}$)/2; dotted black line).

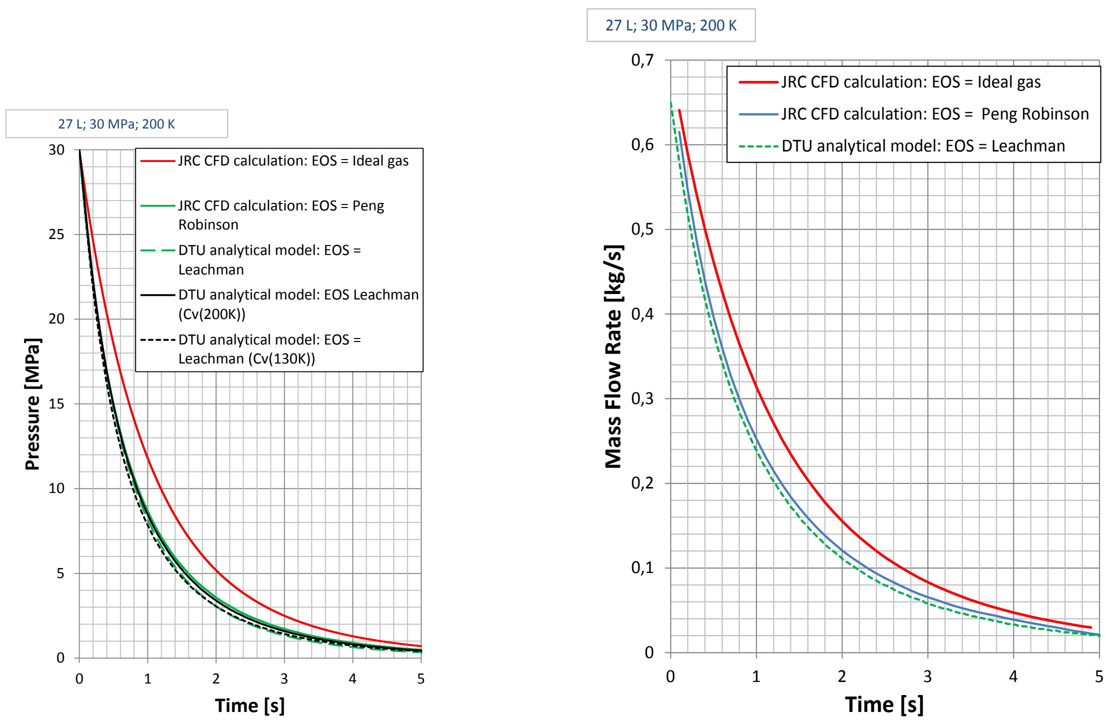

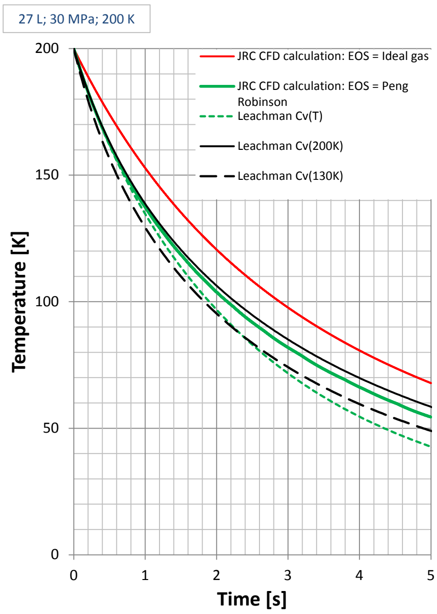


Figure 7. Case 2: Results from the 27L storage release hole radius 3.18mm at 34.5 MPa at 200 K storage temperature.

### 4.3 Case 3: 197 L vessel at low temperature (200 K)

In order to test the basic assumptions made for the engineering model, as e.g. homogeneous pressure and temperature distribution inside the tank the following tests with a 197L vessel are performed using the CFD code from JRC and the engineering model adapted from the yellow book. The hole size radius is 5.7mm and the hydrogen is stored at 30 MPa at 200K.

Simulations are made for the ideal gas release, the CFD code using the Peng Robinson EOS and the engineering model using Leachman's EOS adaption for the compressible factor Z [3,17]. The specific heats are varied: 1) $C_v$ and $C_p$ taken as constant at initial vessel temperature; 2) $C_v$ and $C_p$ taken as constant at $(T_{end}\text{-}T_{start})/2$ and finally 3) as a function of the temperature $C_v(T)$ $C_p$ (T).

The results are shown in Figure 8 for the mass release shows good comparison for the mass flow time dependency though the initial rate for the engineering model is slightly decreased. The decay curve though is close to the one obtained by the Peng-Robinson CFD modeling approach. There are larger differences in the temperature decay, while the pressure decays are in excellent agreement.

### 4.4 Accident consequence

In the case of ignition, a hydrogen release can develop into a jet fires or an explosion depending on the local conditions and on the position and time of ignition. The consequences of those scenarios can be evaluated with simple methods.

An indication on the flame length can be provided by the correlation by Saffers and Molkov [18]. For under-expanded jets like in the case that is investigated in this paper, they developed the following correlation:

$$\frac{L_F}{D} = 805\left[\frac{\rho_N}{\rho_S}\left(\frac{U_N}{C_N}\right)^3\right]^{0.47} \quad for\ \frac{\rho_N}{\rho_S}\left(\frac{U_N}{C_N}\right)^3 > 0.07$$

Where $L_F$ is the flame length, D is the nozzle diameter, $\rho_N$ is the density at the nozzle, $\rho_S$ is the density of the surrounding air, $U_N$ is the flow speed at the nozzle, and $C_N$ is speed of sound at conditions of the gas in the nozzle. For choked flows (M=1) the dimensionless flame length depends only on the hydrogen density in the nozzle $\rho_N$. The density decreases with the decreasing tank pressure and therefore the maximum flame length occurs at the beginning of the release as shown in Figure 9. Since the density is overestimated with the ideal gas equation compared to the real gas equation, also the flame length is larger in the ideal case than in the real case.

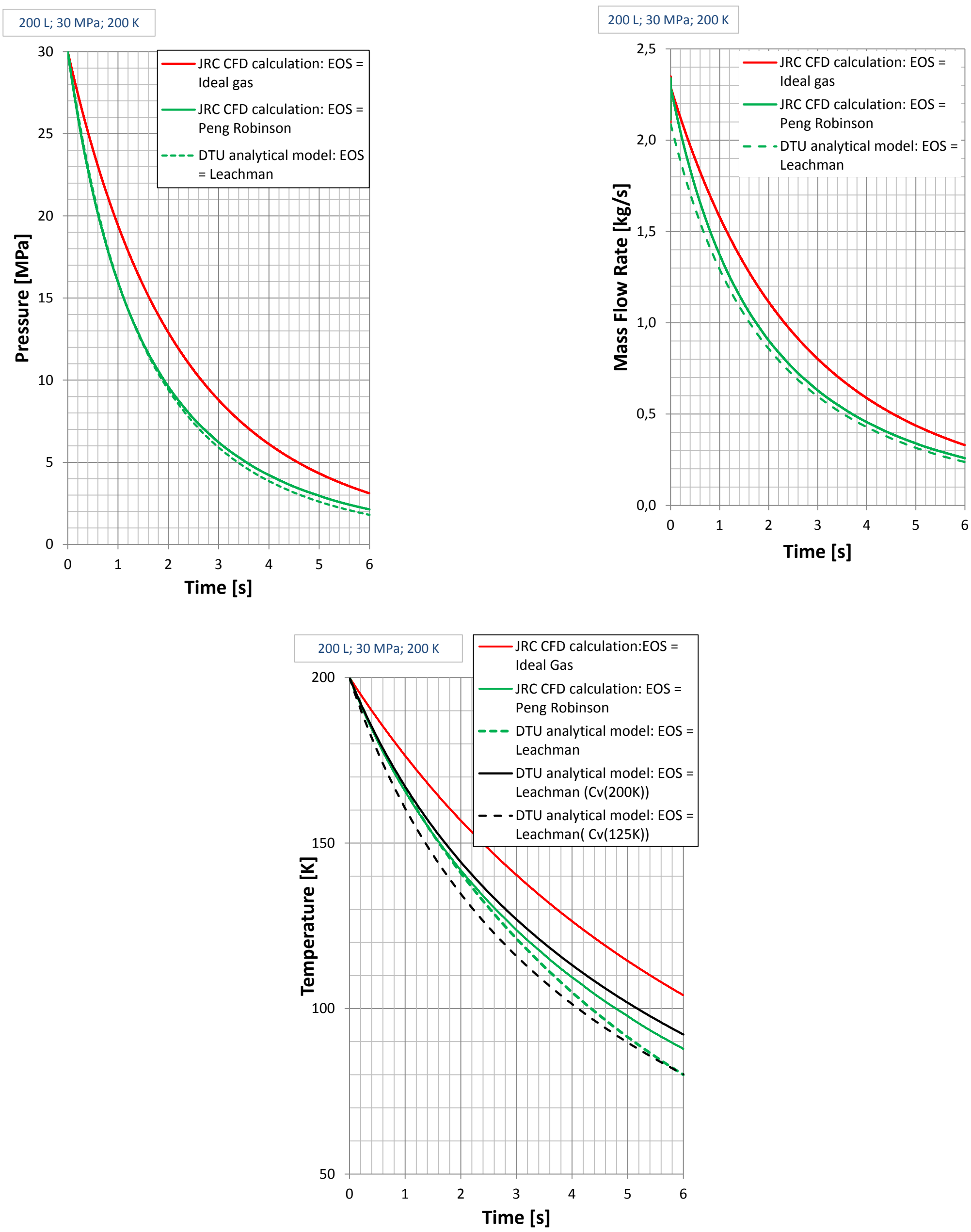


*Figure 8. Case 3: Results for the 197L vessel releases at 30MPa and 200K the hole size radius was 5.7mm*

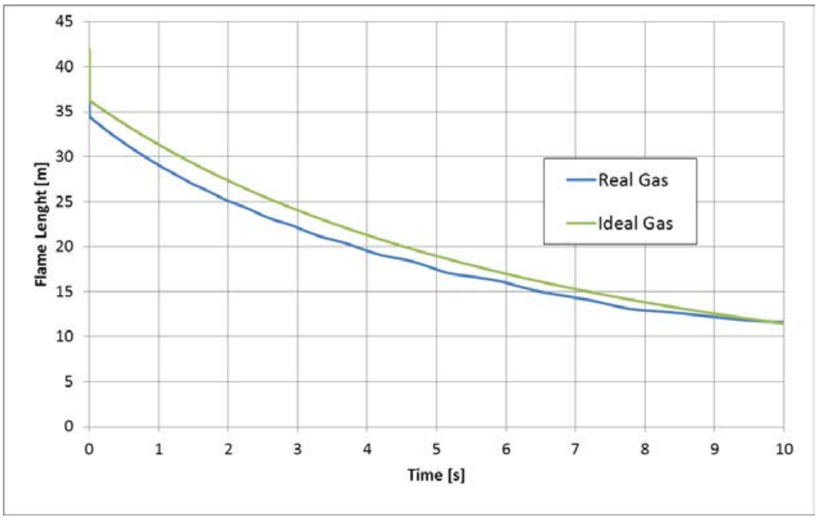


Figure 9: Flame length versus time for the 197L tank. Real gas equation used is the Peng-Robinson EOS.

An evaluation of blast effects and safety distances for unconfined hydrogen explosions can be performed using a simple approximate method that was developed by Dorofeev [11] for that purpose. The main parameter in the model is the total mass of released hydrogen and the worst case conditions of nearly instantaneous releases of hydrogen are assumed. We assume that all the hydrogen in the tank is released as a further conservative condition. Given the different initial density in the real case (26 $kg/m^3$) and in the ideal case (30 $kg/m^3$) for the 197 L tank, the total mass in the ideal case is about 6 kg while it is 5.2 in the real case. Dorofeev defines 3 different levels of congestion (high, medium and low) according to the distance between obstacles and to the size of the obstacles. He also identifies 4 levels of damages to the building: minor structural damage, serious structural damage, partial destruction (50-75%) and total destruction of buildings. If we use Dorofeev's diagrams to provide an approximate conservative indication of the safety distances for the case of high congestion in the real case, the safety distance is about 45 m for the minor structural damage, 17 m for the serious structural damage, 10 m for partial destruction (50-75%) and 7 m for total destruction of buildings. In the ideal case, those distances are about 10% longer.

## 5.0 CONCLUSIONS AND DISCUSSION

The paper describes a modeling approach comparing the use of an engineering numerical model and a CFD outflow model to characterize the hydrogen outflow from a pressurized vessel at ambient and cryogenic temperatures. Different EOS are used to predict the real gas behavior of hydrogen and the results are being compared focusing on the mass release rate, the time profile of the vessel pressure and the time profile of the vessel temperature. The models have been compared to former findings in the literature and excellent agreements are found at ambient conditions using the ideal gas EOS. Real gas EOS, as the reference NIST data, Peng-Robinson, Beattie-Bridgeman and Abel-Nobel [6)], gave also good agreement for the vessel pressure decays. Further, the DTU analytical model and the JRC CFD code are applied to low temperature storage release scenarios at 200K and two vessel sizes of 27L and 197L. The results also show good comparison for the release rates and the pressure time profile, while some more scatter is seen in the temperature time profile of the vessel.

The initial release rates and the duration of the releases are the same for all estimations regardless using ideal or real gas EOS, but the vessel pressure and the release rates decreases much faster with time when using real gas EOS compared to the ideal gas EOS. The ideal gas EOS predicts an unreal high hydrogen density for the initial vessel pressure and thus the total amount of hydrogen released. The uncertainty of the predicted vessel temperature depending on different strategies to estimate the

[6] See appendix A

specific heat $C_v$ input parameter has been investigated. Some larger differences are observed for the calculated vessel temperature time profiles in the low temperature range. By that it appears that the simple approach of using a constant value for the heat capacity is to be questioned for low temperature releases and the specific heat capacity is better modeled as a variable as a function of temperature.

Simple models have been applied to estimate the consequence of the ignition in the case of the release for the 197L tank. The dominant parameter for the flame length is the density at the nozzle and therefore by using the ideal gas law one will overestimate the flame length compared to the estimate with the real gas equation. The strength of an explosion is related to the total amount of mass that is released and therefore to the gas density inside the tank. Since the density is larger with the ideal law than with the real law, also in the case of explosions, by using the ideal law one overestimates the consequence of the accident.

## 6.0 REFERENCES


1. O. Kircher, G. Greim, J. Burtscher, T. Brunner, Validation of cryo-compressed hydrogen storage (CCH2) - A probabilistic approach, (2011).
2. S.M. Aceves, F. Espinosa-Loza, E. Ledesma-Orozco, T.O. Ross, A.H. Weisberg, T.C. Brunner, O. Kircher, High-density automotive hydrogen storage with cryogenic capable pressure vessels, Int J Hydrogen Energy. 35 (2010) 1219-1226.
3. J.W. Leachman, R.T. Jacobsen, S.G. Penoncello, E.W. Lemmon, Fundamental Equations of State for Parahydrogen, Normal Hydrogen, and Orthohydrogen, Journal of Physical and Chemical Reference Data. 38 (2009).
4. A.V. Tchouvelev, Z. Cheng, V.M. Agranat, S.V. Zhubrin, Effectiveness of small barriers as means to reduce clearance distances, International Journal of Hydrogen Energy. 32 (2007) 1409-1415.
5. R.W. Schefer, W.G. Houf, T.C. Williams, B. Bourne, J. Colton, Characterization of high-pressure, underexpanded hydrogen-jet flames, Int J Hydrogen Energy. 32 (2007) 2081-2093.
6. J. Xiao, J.R. Travis, W. Breitung, Hydrogen release from a high pressure gaseous hydrogen reservoir in case of a small leak, Int J Hydrogen Energy. 36 (2011) 2545-2554.
7. E. Papanikolaou, D. Baraldi, M. Kuznetsov, A. Venetsanos, Evaluation of notional nozzle approaches for CFD simulations of free-shear under-expanded hydrogen jets, Int J Hydrogen Energy. 37 (2012) 18563-18574.
8. J.A. Salva, E. Tapia, A. Iranzo, F.J. Pino, J. Cabrera, F. Rosa, Safety study of a hydrogen leak in a fuel cell vehicle using computational fluid dynamics, Int J Hydrogen Energy. 37 (2012) 5299-5306.
9. K. Nasrifar, Comparative study of eleven equations of state in predicting the thermodynamic properties of hydrogen, Int J Hydrogen Energy. 35 (2010) 3802-3811.
10. J.-. Saffers, V.V. Molkov, Towards hydrogen safety engineering for reacting and non-reacting hydrogen releases, J Loss Prev Process Ind. 26 (2013) 344-350.
11. S.B. Dorofeev, Evaluation of safety distances related to unconfined hydrogen explosions, International Journal of Hydrogen Energy. 32 (2007) 2118-2124.
12. Committee for the Prevention of Disasters, Methods for the calculation of physical effects due to the releases of hazardous materials (liquids and gases) 'Yellow Book', CPR 14E (1997).
13. K. Mohamed, M. Paraschivoiu, Real gas simulation of hydrogen release from a high-pressure chamber, International Journal of Hydrogen Energy. 30 (2005) 903-912.
14. R.J. Sadus, Influence of quantum effects on the high-pressure phase behavior of binary mixtures containing hydrogen, J. Phys. Chem. 96 (1992) 3855.
15. ANSYS CFX User's Guide, ANSYS Inc. (2012).
16. Pointwise User Manual. Release 17.0, Pointwise Inc. (2012).
17. E.W. Lemmon, M.L. Huber, J.W. Leachman, Revised Standardized Equation for Hydrogen Gas Densities for Fuel Consumption Applications, Journal of Research of the National Institute of Standards and Technology. 113 (2008) 341-350.

18. V. Molkov, J. Saffers, Hydrogen jet flames, Int J Hydrogen Energy. In press: http://dx.doi.org/10.1016/j.ijhydene.2012.08.106.

## APPENDIX A

The DTU model is based on the described model for vessel dynamics found in the Yellow book. The applied numerical procedure to calculate the vessel pressure, temperature and the realised mass sonic conditions is as follows:

$$
\begin{aligned}
& for\ i\ = 0\ to\ N_t \\
& \qquad t_i = \delta t \times i \\
& \qquad q_i = C_D \cdot A \cdot \Psi \cdot \sqrt{\gamma \cdot \rho_i \cdot P_i \cdot \left(\frac{2}{\gamma+1}\right)^{\frac{\gamma+1}{\gamma-1}}} \\
& \qquad \delta\rho_i = \frac{q_i}{V} \cdot \delta t \\
& \qquad \delta T_i = \frac{P_i}{{\rho_i}^2 \cdot C_v(T_i)} \cdot \delta\rho_i \\
& \qquad T_{i+1} = T_i + \delta T_i \\
& \qquad \rho_{i+1} = \rho_i + \delta\rho_i \\
& \qquad P_{i+1} = Z(P_i, T_{i+1}) \cdot R \cdot \frac{T_{i+1} \cdot \rho_{i+1}}{MM} \\
& \qquad total_{mass_{i+1}} = total_{mass_i} + q_i \cdot \delta t \\
& \qquad break\ if\ P_{i+1} \leq 2 \cdot 10^5 Pa
\end{aligned}
$$

Where $t_i$ – time, s; δt – time step, s; $q_i$ – mass flow rate, kg/s; $C_D$ – discharge coefficient; A – hole area, $m^2$; Ψ = 1- sonic release; γ- $C_p/C_v$; $\rho_i$ – density, kg $m^{-3}$; $P_i$ – vessel pressure, Pa; V – vessel volume, $m^3$; $\delta T_i$ – temperature difference, K; $T_i$ – vessel temperature, K; $C_v$ – isochoric specific heat capacity, J $mol^{-1}$ $K^{-1}$; Z(P,T) – compressibility factor; $R_{gas}$ – gas constant, 8.314 J $mol^{-1}$ $K^{-1}$; MM – molecular weight, 0.002 kg $mol^{-1}$

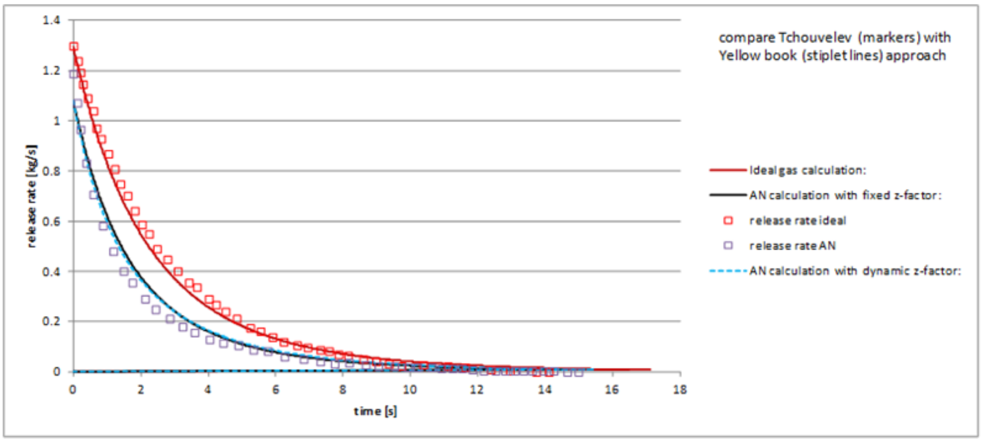


Figure 10. Figure 11Comparison of ideal and AN EOS predictions at 70MPa as published by Tchouvelev et al. [4](squares) with the yellow book model (lines).

Tchouvelev et al. [4] investigated the effects of hydrogen's real gas behaviour using computational fluid dynamics (CFD) modelling techniques. The 60L vessel was initially at 70 MPa, and an accidental hydrogen release impinging horizontally into the wall was assumed. An in-house CFD codes accurately estimated the non-linear hydrogen mass release rate decreasing with time using the PHOENICS software package, both with the ideal gas law and the real gas Abel-Nobel equation of state (AN-EOS).